Experimental investigation on BFRCM confinement of masonry cylinders and comparison with BFRP system

Experimental investigation on BFRCM confinement of masonry cylinders and comparison with BFRP system

Jennifer D'Anna*[1], Giuseppina Amato[2], Jian Fei Chen[3], Giovanni Minafò[1], Lidia La Mendola[1]

[1] *Università degli Studi di Palermo, Dipartimento di Ingegneria, Viale delle Scienze, 90128 Palermo (Italy)*

[2] *School of Natural and Built Environment David Keir Building, Queen's University Belfast (UK)*

[3] *Department of Ocean Science and Engineering, Southern University of Science and Technology, 518055 Shenzhen, China*

***Corresponding author**
jennifer.danna@unipa.it

Abstract

Fabric reinforced cementitious mortar (FRCM) materials have started to be employed during the last years with the aim of overcoming the drawbacks related to the use of fibre reinforced polymer (FRP) composites, proving to be potentially suitable for strengthening masonry structures. Moreover, the will to develop materials able to guarantee a certain degree of sustainability without renouncing to adequate mechanical properties has drawn the attention to the use of basalt fibres, which appear to be a valid alternative to carbon or glass fibres. This work presents an experimental investigation on a basalt FRCM (BFRCM) system to confine circular masonry columns, aimed at evaluating the effectiveness of this system in comparison with data obtained by BFRP jacketing. A total of eighteen clay brick masonry cylinders were prepared by using two different assembling schemes and subjected to uniaxial compression. Six cylinders were tested as control specimens, while the rest were reinforced by using either one or two layers of basalt textile. Traditional measuring instruments were integrated with digital image correlation (DIC) technique. The experimental results are presented in terms of stress-strain curves, and strength and strain enhancements of confined cylinders compared to control specimens. The failure modes are also discussed. All outcomes are compared to those obtained by the authors in a similar study performed on basalt FRP (BFRP)-confined cylinders realized with the same manufacturing in order to have an effective comparison.

Keywords: *Masonry cylinders, Basalt FRCM, Confinement, Strengthening and repair, Digital image correlation (DIC)*

1 Introduction

Fabric reinforced cementitious mortar (FRCM) composite materials are currently receiving great attention as alternative strengthening technique to fibre reinforced polymers (FRPs), especially for masonry elements and when specific preservation criteria need to be fulfilled. Some limitations on the use of FRPs on masonry structures arise due to the low compatibility of epoxy resins or synthetic materials in general when applied to the masonry substrate. The use of

FRCMs allows to alleviate these drawbacks, since the inorganic matrix makes the composite more compatible to the substrate, ensuring durability, also in aggressive environmental conditions, vapour permeability and good resistance to high temperatures. Despite these advantages, some issues are still open about the mechanical properties of FRCM materials and on their effectiveness when adopted in retrofitting techniques. For this reason, numerous recent studies have been performed to investigate the behaviour of FRCM composites in tension [1][2][3][4] and the features of the bond between FRCM and masonry [5][6], as discussed in [7].

In the recent years, experimental studies confirmed the effectiveness of confinement by FRCM for masonry columns. The use of such technique increases the compressive strength of the members and leads to a more ductile failure, with a softer descending behaviour in the post-peak range with respect to unreinforced members. On the other hand, the compressive performance of FRCM-strengthened elements depends on different parameters, such as the adopted fibres and the type of matrix used to apply the textile to the column, but also the kind of confined masonry. Fewer studies were carried out in the literature on the use of FRCMs for masonry confinement in comparison to similar works on FRPs, analytical [8][9][10] or experimental [11][12][13]. One of the first experimental contribution on the FRCM confinement of masonry is that of Di Ludovico et al. (2008) [14], who tested square tuff masonry columns strengthened by glass-grid bonded with a cement-based mortar and subjected to uniaxial compression. Since then, different types of textile have been employed, such as glass [15][16], PBO [17], carbon [18], steel [19], however few studies were performed on the application of natural fibres in composites for structural retrofit. In this field, basalt fibres proved to be a promising alternative to the most common synthetic fabrics, such as carbon or glass fibres, and its development can be useful for the optimization of a retrofit intervention, allowing a reduction of costs with a sustainable and reversible solution. Among the first studies on the confinement by basalt FRCM (BFRCM), Yilmaz et al. (2013) [20] investigated on the efficiency of BFRCM wrapped historical masonry columns, subjected to concentric compressive load. Reinforced specimens showed quite small compressive strength increase (25%) compared to unconfined ones; on the other hand, a significant energy dissipation improvement was attained (86%). The rupture of the basalt fibres at the corners of the columns was observed. As part of larger experimental study, Micelli et al. (2014) [12] tested circular masonry columns confined with continuous and discontinuous BFRCM wraps. Columns confined with discontinuous wraps presented unexpected results, i.e. the strength increase (73%) was higher than that obtained in the case of full-wrapped columns (47%). The authors related this outcome to the double layer of the FRCM jacket and to the scattering typical of masonry material. The failure mode was by tensile rupture of the fibres, accompanied by a diffusive cracking along the height of the column, and the buckling of the cement-based composite jacket was observed. More recently, Mazrea et al. (2016) [21] tested, under compressive load, eighteen BFRCM-confined brick masonry piers with square/rectangular cross-section. Significant axial strain increments were observed, while compressive strength gains

were not so pronounced. Moreover, the confinement was more effective on square masonry piers than on rectangular specimens. Traditional monitoring systems were supported by the use of a digital image correlation (DIC) system, which gave information about the progression of cracks during testing. The effect of masonry strength was investigated by Fossetti and Minafò (2017) [22], by varying the mortar grade of BFRCM-confined clay brick masonry columns. The outcomes showed an average strength increment of 75% for low-grade mortar masonry, while negligible effects were observed in the case of normal strength masonry columns. Santandrea et al. (2017) [23] tested BFRCM-confined square masonry columns, giving particular attention to the influence of the corner radius. The BFRCM jackets provided relatively low compressive strength gain (14-16%) compared to control specimens, due to the brittle failure of basalt fibres at the sharp or rounded corners of the square cross-section columns. Di Ludovico et al (2020) [24] studied the behaviour of full-scale limestone masonry columns strengthened by BFRCM jackets. The results showed an axial strength gain of the confined column of about 45% and the energy dissipation capacity increased of six times respect to the unreinforced specimen. The stress-strain curves presented a softening post-peak branch and, despite the initial strength drop after the peak load, the residual load capacity was close to the peak load of the unconfined column. The spalling of the jacket started at the corners, with the formation of vertical cracks followed by the buckling of the mortar reinforcement in different areas. Ombres and Verre (2020) [25] tested different FRCM systems for the confinement of clay brick masonry columns, among them BFRCM jacketing, showing that this system is able to allow very large lateral displacements at failure. Estevan at al. (2020) [26] performed compressive tests on calcarenite cylinders wrapped by one or three BFRCM layers, comparing the results to those obtained by using other FRCM or FRP systems. Outcomes showed limited strength gains (21%-24%), while the set reinforced with three layers of basalt allowed an ultimate strain increase six times higher than unreinforced masonry, highlighting the suitability of BFRCM system to increase the ductility of masonry columns.

Although the significant number of experimental tests performed during the last decades, a unified analytical approach to describe the compressive response of FRCM-confined masonry columns is still missing in the scientific literature. Numerous analytical formulations have been proposed on the confinement of masonry by FRP [27][28][29][30][31] and, for the sake of brevity, a comprehensive overview can be found in [9]. Some available analytical models on the confinement of masonry by cementitious composites [21][32] are inspired by the models calibrated on FRP-confined members, neglecting the properties of the FRCM, the effect of the matrix, cracking of the jacket, slippage between fibres and matrix. However, the consideration of the matrix role in the prediction of the compressive behaviour of FRCM-confined members appears to be crucial, because it concerns the effectiveness of the FRCM confinement, as shown by Cascardi et al (2017a) [33] that performed a multiple linear regression analysis in order to evaluate the influence of the interaction between the properties of the matrix and those of the fibres on the effectiveness of the

confining pressure. The authors pointed out the need to take into account the matrix characteristics besides those of the fibres in the definition of analytical formulations and proposed a new design-oriented model (DOM) aimed at evaluating the strength increase due to FRCM confinement of masonry. The importance of taking into account the matrix contribution for the definition of proper design formula was evidenced also by Balsamo et al. (2018) [34], who presented a DOM based on the proposal of the Italian CNR-DT 200/2013 [31] code for the FRP confinement of masonry. The accuracy of the proposed equations in predicting the compressive axial strength of FRCM-confined masonry was evaluated by comparison with experimental data. Cascardi et al. (2017b) [35] proposed an analysis-oriented model (AOM) for the definition of the axial stress-strain law of axially loaded FRCM-confined columns made of concrete or masonry and having circular or square cross-section. The model is based on a step-by-step iterative procedure, which adopts the formulations commonly used for classical FRP modelling. More recently, Micelli et al. (2020) [36] proposed a new simplified AOM for the prediction of the stress-strain response of FRCM-confined members. Novel formulas for the computation of both the peak and ultimate axial strains were also proposed and their accuracy was demonstrated by considering an experimental versus theoretical comparison.

Because of the novelty of the strengthening technique and the wide spectrum of FRCM materials (in terms of both grouts and grids) available on the market, as well as due to the variety of existing masonry kinds, further studies are needed to better understand the compressive behaviour of FRCM-confined masonry columns and to derive general design formulations. At the moment, the majority of available experimental works focuses on square/rectangular columns [14]-[25]. Although less common [12][26], the circular section of masonry specimens was chosen in the current investigation in order to study the effect of pure confinement. In fact, the absence of corners in the section allows avoiding stress concentration in the external wrap and, consequently, the strengthening system can reach theoretically its maximum stress in a uniform manner. However, it should be noted that the obtained strength increase can be considered as an upper bound of the confinement effect for real case studies. Moreover, most of experimental works considers specimens reinforced with one or two grid plies [14]-[18],[20]-[24], while the effect of the number of reinforcing layers on the stress-strain response of FRCM-confined columns is investigated only by few studies [25][26], sometimes considering a number of specimens not sufficient to draw general conclusions. Another aspect to be underlined is that the potential of innovative measuring techniques, such as DIC, which has shown to be particularly suitable for the mechanical characterization of FRCM, has been little investigated for the study of the compressive behaviour of FRCM-confined columns, and has been adopted with reference to only square/rectangular columns [21]. Finally, the literature review reveals that a direct and reasonable comparison between the performance of BFRCM and BFRP systems is still missing, which could allow evaluating the reliability of cement-based composites in enhancing the structural performance of masonry columns, in comparison to a more consolidated retrofitting technique, such as the

use of FRP, which involves, however, shortcomings when used on masonry substrate. The effectiveness of BFRCM jacketing, as alternative to BFRP system, could allow several advantages, allowing the achievement of a sustainable and reversible intervention.

The present work is part of a larger study [37] which aims at evaluating the effectiveness, in terms of strength and deformation capacity, of the confinement action provided by both BFRP [38][39] and BFRCM jackets [40], when applied on masonry members. This paper presents the results of a series of compressive tests carried out on small scale brick masonry cylinders strengthened by BFRCM wraps. A preliminary investigation was carried out on the mechanical properties of constituent materials of the masonry and the jacket. Specimens were assembled using two different brick arrangements in order to investigate on the influence of the number of vertical mortar joints. The role of the reinforcing ratio was also studied preparing one and two-layer wrapped specimens. Strains obtained by traditional measuring instruments were compared with those obtained using the DIC technique. The experimental results, presented in terms of full stress-strain curves, compressive strength and strain increments, failure modes, are discussed and compared to the outcomes obtained from identical tests performed on BFRP-confined cylinders, by the authors [38][39], giving interesting information about the effectiveness of BFRCM jacketing as alternative to BFRP.

2 Experimental program

2.1 Specimen construction

Eighteen small clay brick masonry cylinders were assembled and tested under uniaxial monotonic compression. All specimens had a diameter of 94 mm and height of 190 mm, and were produced by coring two different assembly schemes, Scheme I and Scheme II (see Fig. 1). Both schemes were made by three rows of pressed bricks and 8 mm thick mortar joints. Cylinders cored from Scheme I involved only one vertical joint in the middle third (Fig. 1a), while cylinders cored from Scheme II had three staggered vertical joints, one at each level (Fig. 1b). The samples were cored after a curing time of 30 days and then twelve of them were confined with one or two BFRCM layers, while the remaining cylinders were adopted as control samples. A list of all the specimens is presented in Table 1. It should be noted that the same number of specimens was planned to be tested for both schemes. However, the damage of some cylinders during the coring or the preparation operations entailed a different number of specimens for the two schemes. The cylinders were named as CnY_SXL: C means “cylinder”; n indicates the specimen number; Y refers to the matrix used to wrap the cylinders (M means mortar and is used for the cylinders discussed in this paper, R means resin and is used for the cylinders of the companion study [39], while the letter is omitted for unconfined specimens); S indicates

the assembly scheme (W and C for Scheme I and Scheme II respectively); X refers to the number of confinement layers (1 or 2); L stands for “layer”. For unconfined samples, the last two letters were substituted by “Un”.

Table 1: Specimen characteristics

Specimen designation	Brick layup scheme	Number of vertical joints	Number of BFRCM layers
C1_WUn	Scheme I	1	0
C2_WUn			
C3_WUn			
C4_WUn			
C1M_W1L			1
C2M_W1L			
C3M_W1L			
C4M_W1L			
C1M_W2L			2
C2M_W2L			
C3M_W2L			
C1_CUn	Scheme II	3	0
C2_CUn			
C1M_C1L			1
C2M_C1L			
C3M_C1L			
C1M_C2L			2
C2M_C2L			

Fig. 1 Assembly schemes for preparing cylinders: a) Scheme I (wall); b) Scheme II (column)

2.2 Materials

2.2.1 Components of masonry

Pressed bricks with nominal dimensions 50x100x210 mm were used for assembling walls and columns from which the cylinders were cored. In order to characterize the mechanical behaviour of the clay brick units, six 50 mm cubes were tested under uniaxial compression according to EN 772-1 [41]. The bricks had an average compressive strength equal to 42.53 MPa (COV=8.75%).

The mortar used for the masonry cylinders was composed of cement and sand, with a weight ratio of 1/5. Water was added in order to reach the minimum workability. Three-point bending tests were carried out on six standard 40x40x160 mm mortar prisms and uniaxial compressive tests were performed on the obtained twelve halves, according to EN 1015-11 [42]. The mortar had an average compressive strength equal to 20.93 MPa (COV=5.52%) and an average tensile strength of 5.33 MPa (COV=5.13%).

2.2.2 BFRCM system and components

The textile used as internal reinforcement of the composite was a primed alkali-resistant basalt fibre bidirectional grid. According to the technical sheet, the grid had a nominal cell size of 6x6 mm, unit weight equal to 250 g/m^2 and density equal to 2.75 g/cm^3. The equivalent thickness was 0.039 mm and the nominal values of tensile strength, ultimate strain and Young's modulus provided by the manufacturer were f_{fu} = 60 kN/m, ε_u = 1.8%, E_f = 89 GPa, respectively. To characterize the tensile behaviour of the basalt grid, a series of monotonic tensile tests was carried out on textile strips, according to ISO 13934-1 [43]. Twelve strips in the wrap and twelve in the weft direction were cut with dimension 260x13.5 mm and equipped with 80 mm long aluminum tabs at the ends (Fig. 2a), in order to avoid slipping phenomena during testing and to guarantee a uniform load distribution of the applied load. Tensile tests were performed under displacement control by a 100 kN universal machine, using a rate of 2 mm/min. The samples were lighted up with a retrolight and displacements were recorded using the DIC technique, with the support of a videoextensometer able to track linear targets attached to the strips over a gauge length of 80 mm. The recorded average values of strength, strain and Young's modulus are reported in

Table *2*, along with the coefficient of variation (COV). For more details refer to [3][4][37].

A two-component premixed cement-based mortar, enriched with short glass fibres, was used as matrix of the BFRCM system. According to the mechanical characteristics provided by the manufacturer, the mortar had flexural strength of 8 MPa, compressive strength equal to 25 MPa and Young's modulus of 10 GPa. Three-point bending tests were

performed on six standard 40x40x160 mm prisms (Fig. 2b) according to EN 1015-11 [42]. The recorded average flexural strength and COV are reported on

Table *2*.

Additionally, the mechanical behaviour of the composite was characterized under tension (Fig. 2c) [3][4][37]. Fourteen BFRCM coupons were manufactured according to available regulations [44], using different reinforcement ratios. In particular, one series involved eight specimens strengthened with one basalt textile layer, the second series of five specimens was reinforced by two layers and one more specimen was prepared by using three layers. BFRCM coupons were cut from 500x500 mm large slabs, with dimensions 400x40x8 mm, and provided by aluminum tabs on the edges to avoid local damage of the samples inside the clamping area during testing. The front and the thickness side of the strips were painted with a homogeneous layer of white paint and then coated with a random speckle pattern of black paint, defining a grey level distribution adequate for DIC measurements. Specimens were tested using a 100 kN universal testing machine, under displacement control with a speed rate of 0.2 mm/min, adopting the clevis-type grips method. The DIC technique was used to record the strain field. In particular, a high-resolution camera was used to acquire the displacements in the front side of each sample (Fig. 2c) and a videoextensometer was employed to monitor the thickness side in order to detect the possible presence of out-of-plane bending effects [3][4][37]. The specimens were lighted up by mean of artificial lighting to guarantee uniform light distribution.

Table 2: Mechanical characterization of basalt grid and mortar matrix

	BASALT GRID			**MORTAR**
	Average Tensile strength [MPa] and COV	**Average Tensile strain [%] and COV**	**Average Elastic modulus [GPa] and COV**	**Average Flexural strength [MPa] and COV**
Warp	2045 (10.55%)	2.55 (8.21%)	81.91 (3.48%)	7.18 (2.80%)
Weft	1983 (7.80%)	2.40 (12.05%)	81.88 (4.60%)	

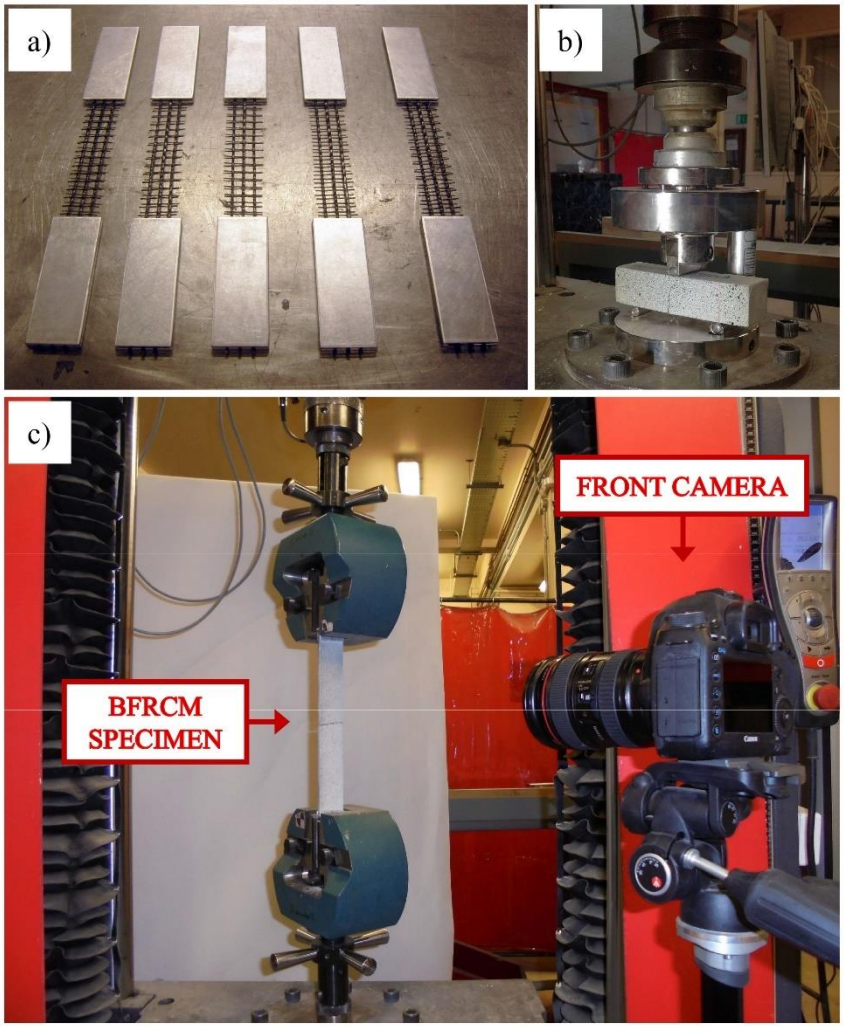

Fig. 2 BFRCM system and components: a) basalt samples; b) three-point bending test on mortar matrix; c) tensile tests on BFRCM composite coupons

2.3 Application of BFRCM jacket

The application of the FRCM jacket involved some sequential steps. In order to ensure good adhesion of the system particular care was taken in the preparation of the substrates, which needed to be perfectly clean and free of crumbling areas or dust. Before applying the products, the specimens were wet in order to have a saturated substrate with a dry surface. The bi-component mortar was prepared by mixing the two components until they were thoroughly blended. Then, an even layer of product of approximately 2 mm was applied on the surface of the specimens by using a flat metal smoothing trowel. While the mortar was still wet, the basalt mesh was placed on the surface and pressed down so that it adhered to the mortar. A second 2 mm thick layer of the same mortar was applied, so that the basalt grid was completely covered. The surface was then smoothed with a smoothing trowel. With the aim to ensure a sufficient bond, the basalt mesh was overlapped for a length equal to 1/3 of the circumference. The specimens were left to cure for more

than one month. During this period, the cylinders were daily wet and covered using drenched gunny clothes covered by plastic sheet in order to ensure an adequate humidity level for the curing of the BFRCM jacket.

2.4 Instrumentation and procedure

A 600 kN electro-hydraulic loading frame was used to perform monotonic compressive tests on the cylinders (Fig. 3a). On each specimen, three loading/unloading cycles were carried out under load control up to 40-50 kN, followed by test to failure under displacement control at a loading rate of 0.002 mm/sec. The axial compression force on the cylinders was applied by a hydraulic jack connected to a manually controlled motor pump. The applied load was measured by a load cell attached to the loading cylinder and recorded by a data acquisition system. In order to guarantee a uniform distribution of axial stress and avoid any eccentricity, a steel spherical head was placed above the upper bearing plate and centered with the specimen.

A total of six linear voltage differential transducers (LVDTs) were installed, four to monitor the displacement of the upper loading platen and two on the lower platen. In order to measure the local axial strain in the middle half of the specimens, three extensometers connected to two steel rings placed around the cylinders were also used (Fig. 3b).

Furthermore, the DIC technique was used to analyze the strain field on the surface of the cylinders during compressive tests. For this purpose, cylinders were painted with a high-contrast texturing effect using white paint with black spackle pattern. A 22.3 Megapixel camera was used to record images of the specimens every four seconds using a remote trigger, with a resolution of 16 pixel/mm. The camera was positioned in front of the testing machine, perpendicular to the cylinder surface, with the lens directed towards the centre of the sample Fig. 3a. In the case of confined cylinders, it was ensured that the specimens were positioned in order to have the camera opposite to the FRCM overlap. The specimens were lighted up using two symmetrical white lights, able to provide a uniform light intensity on the front side of the samples (Fig. 3a). The software GOM Correlate [45] was used to process the images acquired during compression tests on the masonry cylinders.

Strains were measured over a rectangular area of about 50x90 mm, as shown in Fig. 4, as in [46]. Axial strains were computed as the average of 20 virtual strain gauges with a gauge length of 90 mm. In the same way, hoop strains were measured as the average of 45 virtual strain gauges with a gauge length of 50 mm.

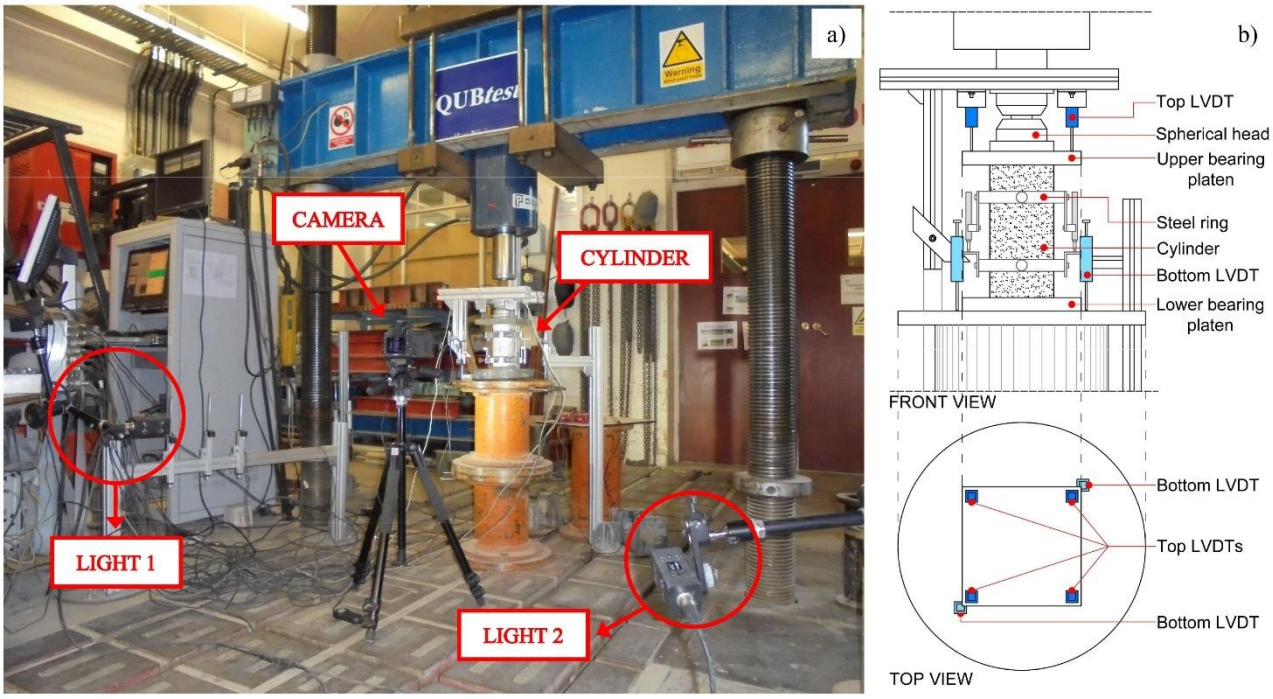

Fig. 3 Compressive tests on masonry cylinders: a) overall setup; b) setup scheme

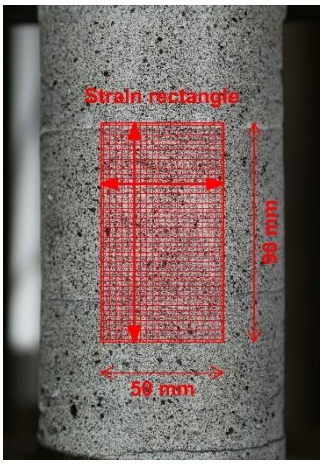

Fig. 4 Strain rectangle used to measure hoop and axial strains (DIC)

3 Experimental results and discussion

3.1 BFRCM system

The results of tensile tests on BFRCM coupons are reported in Fig. 5a in terms of load-strain curves. In general, for each curve it is simple to recognize the three stages typical of the tensile behaviour of FRCM composites. The first stage (Stage I) is characterized by a linear response up to the achievement of the tensile strength of the mortar, which determines the formation of the first crack. Stage II is characterized by consecutive load drops, due to the development of cracks in the matrix, and by a stiffness reduction. Once the crack pattern has fully developed, a regain in stiffness is

observed and the growing applied displacement produces a nearly linear load increase (Stage III). This stage ends when the load bearing capacity of the composite material is reached.

Table 3 reports the average experimental results in terms of peak load (F_I, F_{II}, F_{III}), peak stress (σ_I, σ_{II}, σ_{III}) and corresponding strain (ε_I, ε_{II}, ε_{III}) related to the three characteristic points at the end of each stage, for the three series of samples. The tangent moduli corresponding to the three stages are also listed. In terms of maximum load, it is evident that the specimens reinforced with two and three layers showed higher bearing capacity compared to one-layer coupons, with a progressive load increase from Stage I to Stage III. On the other hand, in terms of stress, results point out a progressive reduction of the values related to the characteristic points for over-reinforced specimens. Regarding the strain values, the average strains at the end of Stage I for the three series of specimens are quite similar. Conversely, with the increase of the reinforcing ratio, a progressive strain decrease was detected at the end of both Stage II and Stage III.

Fig. 5b presents the crack pattern at failure for three specimens reinforced with one, two and three layers, respectively. The failure of BFRCM coupons was always characterized by the tensile rupture of the basalt grid, after a homogeneous cracking along the length of the specimens. The images show that the cracks are well widespread along the surface of the coupons, underlining the good ability of the basalt mesh to transfer load to the matrix. The increase of the number of reinforcing layers gave rise to a larger number of cracks, progressively closely spaced. DIC technique allowed a deep analysis of the full crack development over the surface of the strips and more details can be found in [3][4][37].

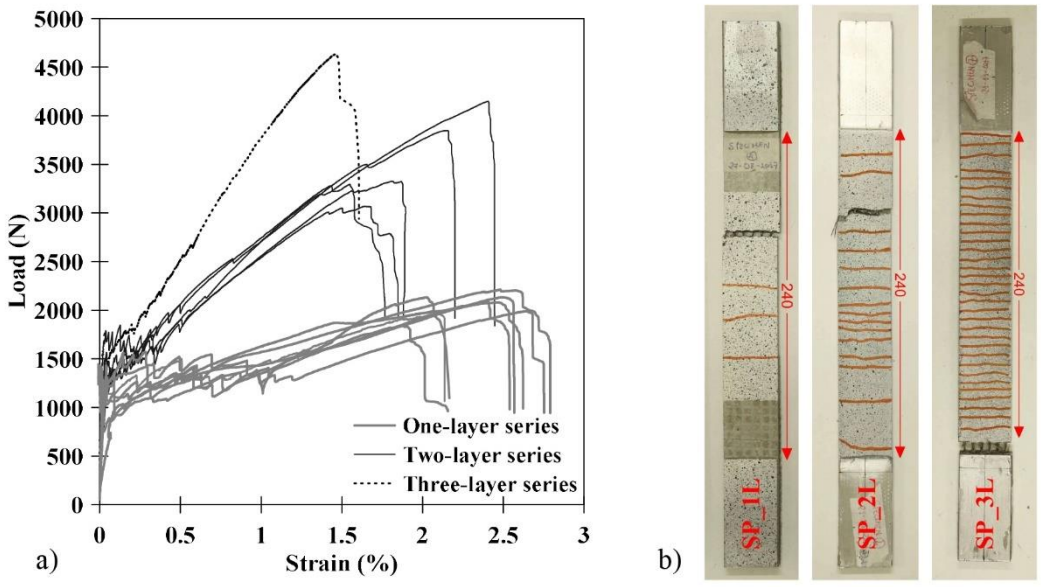

Fig. 5 Tensile tests on BFRCM composite coupons: a) load-strain curves of the three series; b) one, two and three-layer reinforced specimens after testing

Table 3: Average results of tensile tests on BFRCM coupons

Series	Stage	Peak load [kN]	Peak stress [MPa]	Strain [%]	Tangent modulus [GPa]
		F	**σ**	**ε**	**E**
SP_1L	I	1234.11	881.50	0.030	3309.50
	II	1398.03	998.60	1.019	17.01
	III	2054.93	1467.28	2.322	37.25
SP_2L	I	1448.22	517.22	0.035	1664.35
	II	1855.26	662.59	0.448	36.51
	III	3538.20	1263.64	1.912	40.90
SP_3L	I	1437.38	342.23	0.044	786.74
	II	1821.68	433.73	0.229	43.78
	III	4633.19	1103.14	1.466	54.13

3.2 BFRCM-confined cylinders

The axial stress-strain results of compressive tests on unconfined and BFRCM-confined cylinders are presented in Fig. 6, for Scheme I and Scheme II respectively, using readings from external LVDTs and local transducers. The axial strain up to the peak was obtained considering the displacement recorded over the central half of the cylinders. The LVDTs placed at top and bottom plates were used instead to plot the post-peak branch, since the rings fixed on the cylinders had to be taken off during the last part of the tests. For unconfined cylinders C1_WUn, C2_WUn, and C3_WUn the readings in the central area of the specimens were lost during testing, thus the strain was fully evaluated using the external LVDTs on the top and bottom plates. It should be noted that the stiffness obtained in this way is likely lower than the actual stiffness of the specimen (see Fig. 6a and b), so it may be used as reference only. For this reason, the strains of these cylinders were excluded for the calculation of the average strain of unconfined specimens.

The unconfined cylinders show a brittle behaviour, characterized by an almost linear ascending branch up to the peak and a steep load drop after the peak (Fig. 6). The stress-strain curves of BFRCM-confined cylinders present a linear behaviour up to the development of the first crack in the external jacket, which coincide with the failure of the inner masonry core. This is clearly detectable from the curves, which experience a limited stress drop. Afterwards, the curves show a new stress increase due to the activation of the jacket because of the lateral expansion of the crushed masonry core. This new stress increment develops up to the peak, with a less stiff trend than the initial one. After the maximum stress is reached, a quite steep descending branch can be detected, with a sudden drop in strength due to the basalt grid damage. Afterwards, the stress decrease starts to show a smoother trend: at this point the mesh was already broken in some parts, but the jacket could still guarantee a certain degree of ductility. The post-peak drop is quite pronounced for both Scheme I and Scheme II cylinders. All the specimens show an almost bilinear softening branch characterized by a steep strength decrease followed by a plateau region, with considerable values of residual strength, particularly in the case of two-layer wrapped specimens from Scheme I. On the other hand, there are not considerable differences in the

softening behaviour of Scheme II cylinders wrapped with one or two basalt grid layers. Note that the full stress-strain curve of the cylinder C3M_W2L is not available because of a technical issue during testing. In particular, in Table 4 the compressive strength value is reported, but the corresponding strain is missing.

In Table 4 the individual experimental results of unconfined and confined cylinders are reported in terms of peak stress (f_{m0} - f_{mc}), axial strain at peak stress (ε_{m0} - ε_{mc}) and ultimate axial strain corresponding to a 15% stress reduction with respect to the peak value (ε_{mu} - ε_{mcu}), along with the average values and the COVs. For unconfined cylinders from Scheme I, the ultimate axial strain is the last detected value.

Table 5 provides the strength and strain increments of confined cylinders compared to unconfined cylinders.

In the case of unconfined cylinders, the average peak stress values were 25.19 MPa and 19.85 MPa for Scheme I and Scheme II respectively, pointing out a considerable detrimental effect of the vertical mortar joints. For one-layer confined cylinders, the average strength increases were equal to 27% and 66% for Scheme I and Scheme II specimens respectively, compared to unconfined cylinders. Two layers of BFRCM produced an average strength enhancement of 38% for Scheme I and 85% for Scheme II cylinders. Comparing specimens reinforced with one and two layers, the strength gain was of 9% and 11% for Scheme I and Scheme II respectively. As expected, the effectiveness of BFRCM confinement was higher for the weakest masonry, namely in the case of Scheme II cylinders having three vertical joints.

Results showed an increase of the strain at peak stress of BFRCM-confined specimens. One-layer reinforced cylinders from Scheme I and Scheme II exhibited an average increase equal to 59% and 45 % respectively, respect to unconfined cylinders. Regarding two-layer confined specimens, Scheme I showed an average increase of 72%, while specimens from Scheme II presented an average strain gain of 75%.

Regarding the ultimate strain, Scheme I cylinders showed an average ultimate strain gain of 94% and 122% for one and two layers respectively, in comparison to unconfined samples. For cylinders from Scheme II, the increments were 96% and 121% for specimens wrapped with one and two layers respectively.

Moreover, Scheme I cylinders exhibited an average ultimate axial strain increase of 29% and 37% than the peak strain for one and two layers respectively. The same increments for Scheme II cylinders were equal to 52% and 41%.

Table 4: Test results of BFRCM-confined masonry cylinders by using LVDTs/Transducers

	Specimen designation	BFRCM layers	Peak axial stress (MPa)	Average and COV	Peak axial strain [mm/mm]	Average and COV	Ultimate axial strain [mm/mm]	Average and COV
			f_{m0}		ε_{m0}		ε_{mu}	
UNCONFINED	C1_WUn	-	25.24	25.19 17.60%	0.0043*	0.0036 12.41%	0.0048*	0.0038 15.91%
	C2_WUn	-	24.78		0.0052*		0.0054*	
	C3_WUn	-	19.95		0.0049*		0.0049*	
	C4_WUn	-	30.79		0.0036		0.0038	
	C1_CUn	-	22.25	19.85 17.14%	0.0036	0.0034 8.88%	0.0042	0.0038 13.56%
	C2_CUn	-	17.44		0.0032		0.0035	
			f_{mc}		ε_{mc}		ε_{mcu}	
BFRCM CONFINED	C1M_W1L	1	25.25	32.04 (17.40 %)	0.0045	0.0058 (21.27 %)	0.0072	0.0074 (13.37 %)
	C2M_W1L	1	35.73		0.0068		0.0083	
	C3M_W1L	1	37.38		0.0068		0.0081	
	C4M_W1L	1	29.80		0.0050		0.0061	
	C1M_W2L	2	33.84	34.78 (10.35 %)	0.0061	0.0062 (2.75 %)	0.0081	0.0085 (6.76 %)
	C2M_W2L	2	31.75		0.0064		0.0089	
	C3M_W2L	2	38.76		/		/	
	C1M_C1L	1	30.81	32.98 (9.60 %)	0.0058	0.0050 (18.78 %)	0.0078	0.0075 (7.07 %)
	C2M_C1L	1	36.61		0.0051		0.0069	
	C3M_C1L	1	31.52		0.0040		0.0079	
	C1M_C2L	2	39.22	36.73 (9.58 %)	0.0065	0.0060 (12.16 %)	0.0079	0.0085 (8.90 %)
	C2M_C2L	2	34.24		0.0055		0.0090	

*Results not used for the calculation of the average peak and ultimate strain.

Table 5: Strength and strain increments for BFRCM-confined cylinders

Assembly	Confinement	f_{mc}/f_{m0}	$\varepsilon_{mc}/\varepsilon_{m0}$	$\varepsilon_{mcu}/\varepsilon_{mu}$	$\varepsilon_{mcu}/\varepsilon_{mc}$
Scheme I	1 layer	1.27	1.59	1.94	1.29
	2 layers	1.38	1.72	2.22	1.37
Scheme II	1 layer	1.66	1.45	1.96	1.52
	2 layers	1.85	1.75	2.21	1.41

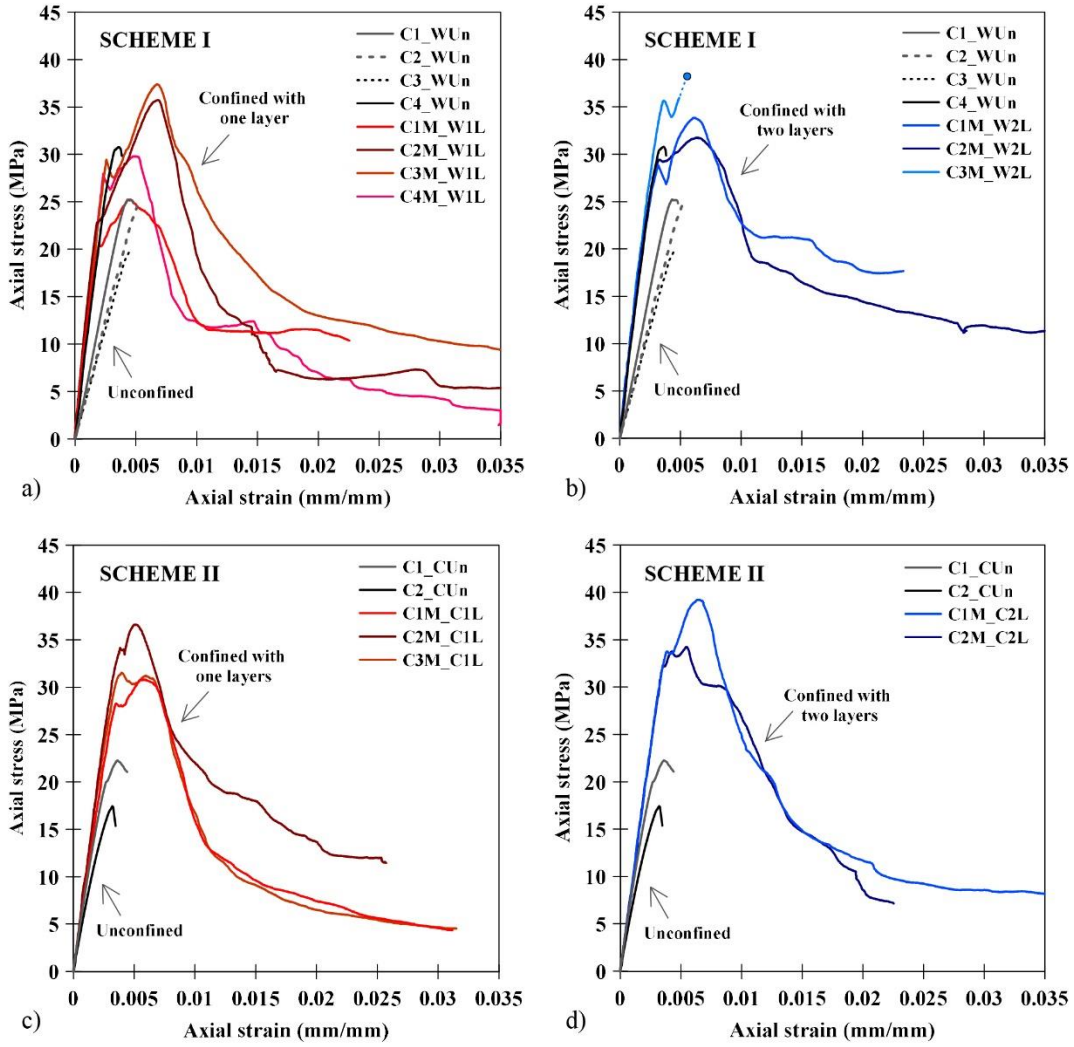

Fig. 6 Axial stress-strain curves of BFRCM-confined cylinders plotted by using readings of LVDTs: a) Scheme I – one layer; b) Scheme I – two layers; c) Scheme II – one layer; d) Scheme II – two layers

The axial and hoop stress-strain curves obtained by DIC measurements are plotted in Fig. 7 and Fig. 8 for Scheme I and Scheme II cylinders respectively, along with results from LVDTs. DIC was not used for four unconfined cylinders (C1_WUn, C4_WUn, C1_CUn and C2_CUn) and for one-layer reinforced specimens from Scheme I.

The comparison points out that along the ascending branch, readings of DIC are close to those of LVDTs and in general stiffer. In the case of confined cylinders, the axial stress-strain curves (LVDTs and DIC) of each specimen match each other pretty well up to the first load drop, which coincides with the start of crack development over the FRCM jacket. After this point, for some specimens (C3M_C1L, C1M_C2L) there are inconsistencies in the strain readings of the two acquisition systems. This can be explained considering that the digital system measured over a limited zone of the cylinder surface (90x50 mm) and the vertical deformations occurred on the wrapped surface (i.e. on the confinement layer) were gauged directly. On the other hand, the local transducers connected to the steel rings and the external LVDTs placed at top and bottom of the cylinders measured vertical displacements without contact with the jacket; moreover, external LVDTs, used to plot strains after the peak, measured global displacements with a gauge length equal

to the cylinder length. Furthermore, during the development of the test, the jacket started to crack and the external layer of mortar started to separate from the masonry core in certain areas. Thus, it is possible to conclude that whereas DIC results describe the behaviour of the external wrap, measurements of LVDTs represent the overall behaviour of the specimen. As a result, because of the differences in gauge length, the measuring location (on the jacket for DIC and between rings/plates for the transducers) and the detachment of the jacket from the core, some differences between the two measurements could not be avoided.

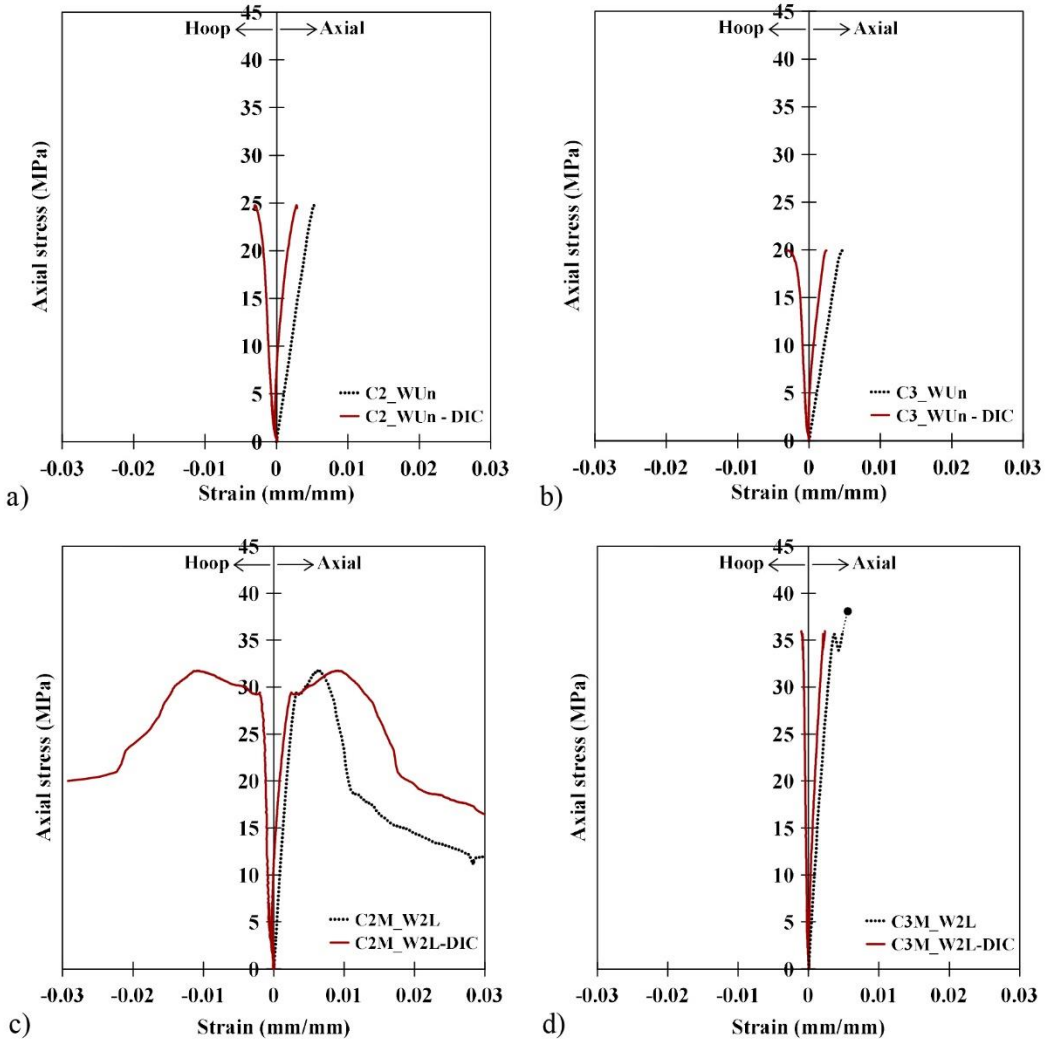

Fig. 7 Stress-strain curves in the axial and hoop direction for Scheme I cylinders, plotted by using DIC and LVDTs: a) b) unconfined; c) d) confined with two layers

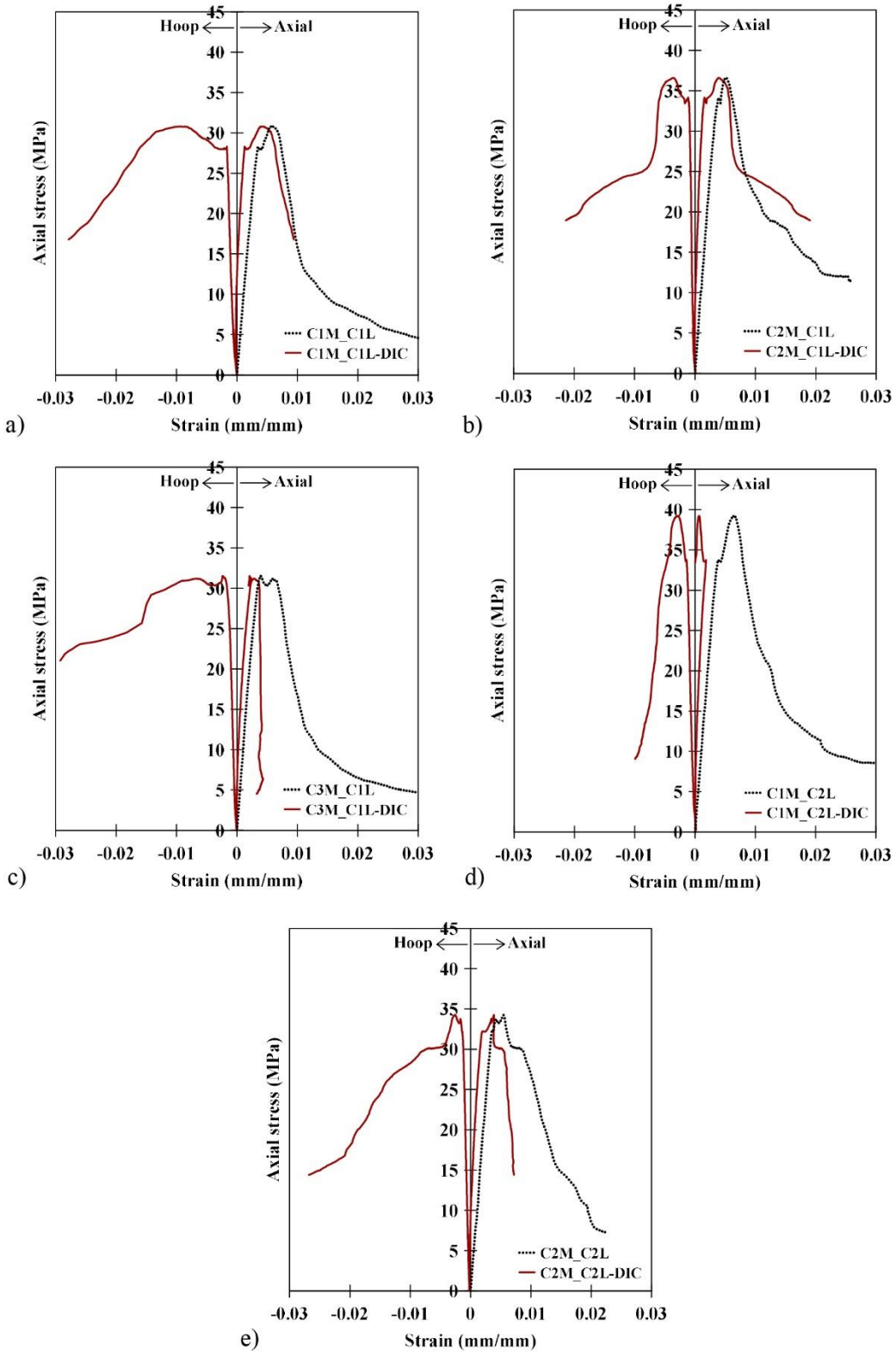

Fig. 8 Stress-strain curves in the axial and hoop direction for Scheme II cylinders, plotted by using DIC and LVDTs: a) b) c) confined with one layer; d) e) confined with two layers

3.3 Failure modes of masonry cylinders

Fig. 9 shows unconfined and BFRCM-confined cylinders at the end of the compression tests. As expected, the unconfined specimens showed a brittle behaviour and the failure was characterized by the formation of large and almost vertical cracks along the height. Not substantial differences were observed in the failure mode of Scheme I and Scheme II cylinders. Vertical joints created preferential routes for the development of cracks, which propagated at brick-mortar interface. This behaviour was more evident for Scheme II specimens having three vertical joints and less for Scheme I, which involved also cracks in bricks. The failure involved crushing of masonry with spalling of material for whole the height of the cylinders. In particular, large portions of bricks between mortar joints were detached from the cylinders (see Fig. 9a and b).

Regarding confined cylinders, there were not marked differences in the failure mode of different schemes (Fig. 9c-e) and the ultimate condition was reached by failure of the basalt mesh at cracks developed in the mortar of the jacket (Fig. 9g). The crack pattern was characterized by vertical cracks that developed for the entire length of the samples, producing the detachment of the external mortar layer of the jacket in those parts and the loss of material in some areas. Apart of these zones, the jacket was solid, with the grid and the two mortar layers very tight, and it was well linked to the inner masonry core. At failure, the masonry core was severely crushed (see Fig. 9f).

Fig. 9h shows the failure mode of a representative BFRP-confined cylinder (C2R_C1L), tested by the authors in a previous companion study [39]. In the case of BFRP wrapping, the cylinders were characterized by two or more almost vertical cracks and the specimens failed for the tensile rupture of the BFRP jacket, as happened for BFRCM confinement. Crushed masonry could be observed at the end of the test inside the jacket. However, BFRP-confined cylinders showed a brittle failure, due to the brittle behaviour of FRP, and the jacket broke in defined zones of the specimens. On the contrary, there was not neither a brittle failure nor a clear failure point for BFRCM-confined specimens.

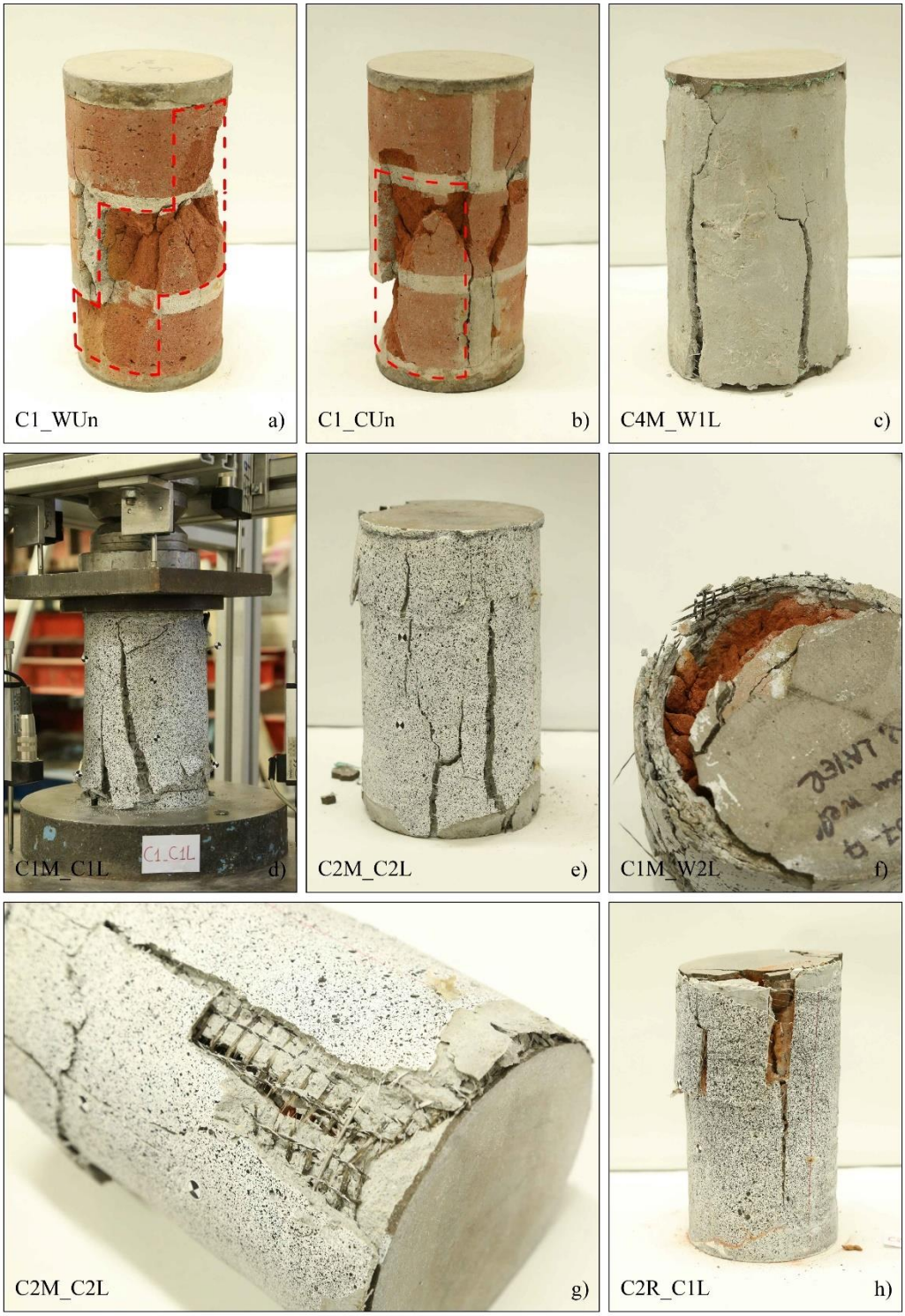

Fig. 9 Failure mode of cylinders: a) Scheme I, unconfined; b) Scheme II, unconfined; c) Scheme I, 1 layer of BFRCM; d) Scheme II, 1 layer of BFRCM; e) Scheme II, 2 layers of BFRCM; f) severely crushed masonry core; g) failure of BFRCM jacket; h) Scheme II, 1 layer of BFRP

3.4 Comparison between the performance of BFRCM and BFRP confinement

Aiming at comparing the strengthened system studied in this work with a more consolidated retrofitting technique, reference is made to an experimental work carried out by the authors on BFRP-confined masonry. In a previous companion study [39], the authors tested the same clay brick masonry cylinders confined by BFRP wraps, using the same basalt grid used in this work. In this section, results from compressive tests on BFRCM and BFRP-confined cylinders are compared in terms of stress-strain curves, and strength and strain increments.

In Fig. 10 the axial stress-strain curves of BFRCM and BFRP-confined cylinders belonging to the same scheme and strengthened with the same number of layers are depicted. The strength and strain increments of confined cylinders compared to unconfined cylinders, for both BFRCM and BFRP-confined specimens, are reported in Fig. 11, which includes also the ratio between ultimate and peak axial strain of confined cylinders.

In general, it is clear that both the strengthening systems are able to improve the bearing capacity of the masonry, with the peak stress increasing with the increase of the reinforcing layers. Considering Scheme I cylinders confined with one layer, the strength increase with respect to unconfined specimens was comparable for BFRCM and BFRP-confined cylinders (27% and 29%, respectively), while two layers of BFRP (68% increase) were more effective than two layers of BFRCM (38% increase), see Fig. 11a. However, it should be noted that three specimens were tested by using two BFRCM plies and only two samples by using BFRP. Thus, differences observed in the strength increases should be revised by testing the same number of specimens. Despite the different strength gain, it is evident that BFRP confinement induced a more brittle behaviour with respect to BFRCM (Fig. 10a and b). In fact, the stress-strain curves of BFRP-confined specimens of Scheme I show a steep post-peak branch, which reflects the failure mode of the cylinders. On the contrary, BFRCM-wrapped specimens exhibit a more ductile softening, with greater values of residual strain.

Analogously, BFRCM and BFRP-confined cylinders of Scheme II showed a different behaviour in terms of strength increase, with higher increments yielded by BFRCM respect to BFRP, for both one (66% vs 38%) and two layers (85% vs 71%) of reinforcement (Fig. 11a).

It should be noted that the effectiveness of the confinement was higher for Scheme II (weaker masonry involving three vertical mortar joints), for both BFRP and BFRCM-confined specimens. The number of the joints, however, had a stronger effect in the case of BFRCM-confined cylinders (Fig. 11a). Indeed, considering BFRP-confined cylinders from Scheme II, the strength gains of one and two-layer reinforced samples were greater of 31% and 4% respectively, compared to the strength gains of Scheme I cylinders. On the other hand, for BFRCM-confined cylinders from Scheme II, the strength increases of one and two-layer strengthened samples were greater of 144% and 124% respectively,

compared to the strength gains of Scheme I samples. The strength increases due to the addition of a second layer were more pronounced for BFRP-confined cylinders (Fig. 11a), with increments of 134% and 87% for Scheme I and Scheme II respectively, while the same increments for BFRCM-wrapped cylinders were equal to 41% and 29%.

Other experimental studies pointed out that FRCM jacketing is able to guarantee compressive strength increases comparable to those achieved by using FRP, when employing glass or carbon fibres [47][48]. On the other hand, available outcomes on the confinement of masonry by BFRCM [26] evidenced limited strength gains (up to 26%), while considerable improvements of ductility were registered for the strengthened samples. It is worth to note that, in the literature, a direct comparison between the performance of BFRP and BFRCM is still missing. Thus, the results obtained in the present work are of paramount importance, but need to be integrated with additional experimental investigations.

Regarding the average peak strain increments (Fig. 11b), for Scheme II the two strengthened systems produce comparable gains with respect to unconfined specimens, with slightly better results for the BFRP system when using one layer (45% vs 49%) and slightly better results for the BFRCM system with two layers (75% vs 69%). For Scheme I, BFRCM wrapping is more effective than BFRP wrapping for one layer, with strain increments of 59% and 17%, respectively, while for two layers the strain gains are comparable (72% vs 82%).

Considering the average ultimate strain gains, BFRCM system is more effective than BFRP for Scheme I cylinders wrapped with one (94% vs 46% of increase) and two layers (122% vs 104% of increase). For Scheme II, one layer of BFRCM or BFRP produces comparable results, with strain gains of 96% and 93% respectively, while the BFRP system is more effective for two-layer wrapped samples (121% vs 146% of increase).

In Fig. 11d to the average ratio between ultimate and peak strains of confined cylinders is reported in order to measure the ductility gains. The best results are achieved in the weaker masonry (Scheme II), for both BFRCM and BFRP system, with gains of 52% and 45% respectively for one-layer reinforced cylinders, and gains of 41% and 62% for two-layer confined cylinders. For Scheme I, similar increments are achieved with one layer of BFRCM (29%) and BFRP (33%), while two layers are more effective using BFRCM than BFRP (37% vs 20%).

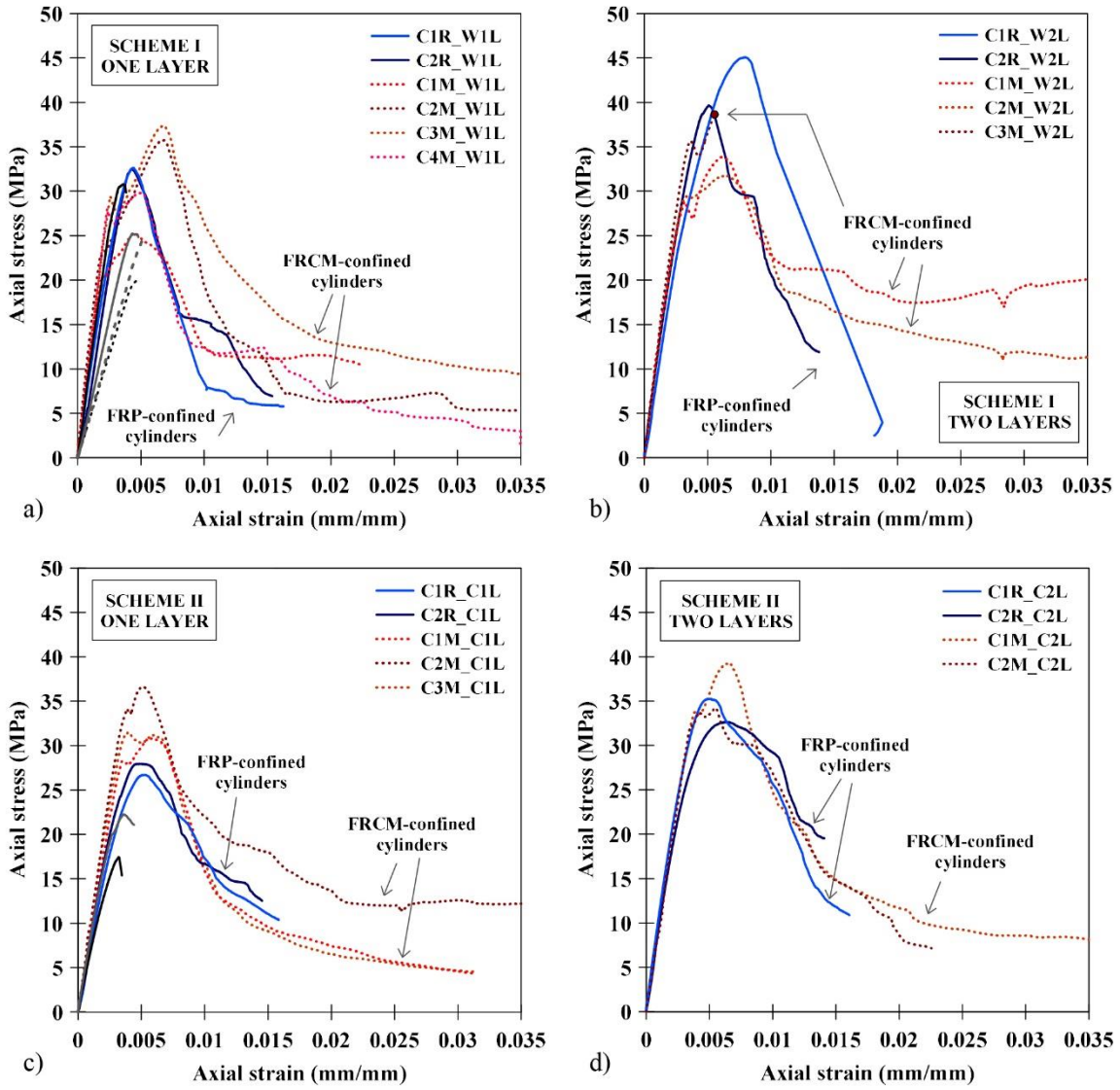

Fig. 10 Axial stress-strain curves of confined cylinders: a) one-layer reinforced specimens of Scheme I; b) two-layer reinforced specimens of Scheme I; c) one-layer reinforced specimens of Scheme II; d) two-layer reinforced specimens of Scheme II

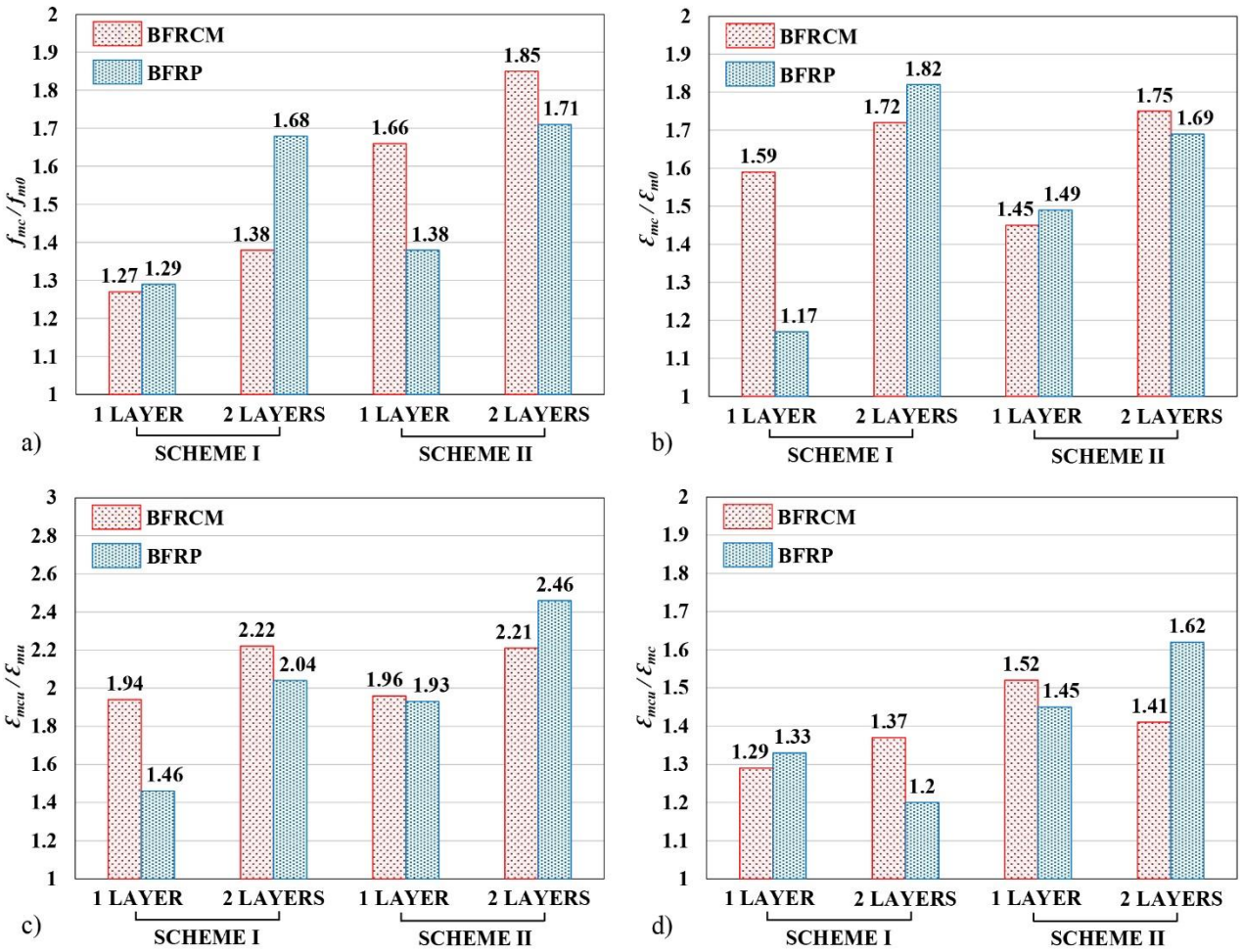

Fig. 11 Comparison of average increments for BFRCM and BFRP-confined cylinders: a) strength increments; b) peak strain increment; c) ultimate strain increment; d) increment of ultimate strain respect to peak strain

Conclusions

This paper presented the results of an experimental study on small scale clay brick masonry cylinders confined by BFRCM wraps. The outcomes were compared with the experimental results of analogous tests performed by the authors on BFRP-confined cylinders. Based on the experimental analyses in the previous sections, the following conclusions can be drawn:

- Unconfined cylinders with three vertical mortar joints (Scheme II) presented an average strength about 20% lower compared to cylinders with one vertical joint (Scheme I);
- The ultimate condition of BFRCM-confined specimens was reached by tensile failure of the basalt textile, highlighting that the full capacity of the fabric was exploited. At failure, the inner masonry core of wrapped cylinders was crushed;
- The BFRCM composite considerably increased the strength of the confined cylinders, with gains of 27% and 66%

for one-layer reinforced specimens from Scheme I and II respectively, compared to control samples; strength gains of two-layer confined specimens were 38% and 85% for Scheme I and II respectively;

- Regarding the strain at peak stress, one-layer reinforced cylinders from Scheme I and Scheme II exhibited an average increase of 59% and 45% respectively, compared to control specimens. Two-layer confined cylinders showed gains of 72% and 75% for Scheme I and Scheme II, respectively;
- Masonry cylinders confined by BFRCM exhibited a ductile behaviour, with a softening post-peak branch and considerable values of residual strength, particularly for two-layer wrapped cylinders from Scheme I;
- Results from transducers and DIC match each other quite well up to the crack development over the FRCM jacket. Because of the different measuring location, differences in gauge length, cracking and detachment of the jacket from the masonry core, some differences between the two measurements could not be avoided. DIC describes the behaviour of the external jacket, while measurements of LVDTs represent the overall response of the specimens;
- The comparison between BFRCM and BFRP systems showed that the BFRCM can guarantee strength and ductility gains comparable to those obtained by using BFRP. The strength gains were higher for BFRCM system than BFRP, in the case of Scheme II, for both one- and two-layer confined cylinders. In general, results in terms of strain gain are comparable for the two strengthening systems and, in the case of considerable difference, the BFRCM gives better results;
- Overall findings and the comparison with results obtained from compressive tests on BFRP-wrapped masonry underline that the BFRCM confinement can be considered an effective solution to improve the mechanical features of brick masonry cylinders, coupling the advantages of basalt fibres (reduced costs and low environmental impact) with those of the cementitious matrix (higher compatibility with masonry substrate). This is of paramount importance for future retrofit interventions.
- The influence of other parameters, such as kind of masonry, shape of cross-section, type of cementitious matrix, on the effectiveness of the studied strengthening system needs to be investigated. Moreover, the study should be extended to the case of large-scale columns to understand the possible occurrence of scale effects.

References

[1] Caggegi C, Lanoye E, Djama K, Bassil A, Gabor A. Tensile behaviour of a basalt TRM strengthening system: influence of mortar and reinforcing textile ratios. Compos Part B-Eng 2017; 130: 90-102.

[2] Ferrara G, Pepe M, Martinelli E, Tolêdo Filho RD. Tensile behavior of Flax Textile Reinforced Lime-Mortar: Influence of reinforcement amount and textile impregnation. Cem Concr Compos 2021; 119: 103984.

[3] D'Anna J, Amato G, Chen JF, Minafò G, La Mendola L. On the use of Digital Image Correlation (DIC) for evaluating the tensile behaviour of BFRCM strips. In: Key Engineering Materials 2019. Vol. 817, p. 377-384. Trans Tech Publications Ltd.

[4] D'Anna J, Amato G, Chen JF, Minafò G, La Mendola L. Experimental application of digital image correlation for the tensile characterization of basalt FRCM composites. Constr Build Mater 2021; 271: 121770.

[5] Dalalbashi A, Ghiassi B, Oliveira DV, Freitas A. Fibre-to-mortar bond behaviour in TRM composites: effect of embedded length and fibre configuration. Compos Part B-Eng 2018; 152: 43-57.

[6] Bellini A, Bovo M, Mazzotti C. Experimental and numerical evaluation of fibre-matrix interface behaviour of different FRCM systems. Compos Part B-Eng 2019; 161: 411-426.

[7] Amato G, Chen JF, D'Anna J, La Mendola L, Minafò G. (2017, September). FRCM systems for strengthening masonry structures. In: Proceedings of the 8th Biennial Conference on Advanced Composites in Construction. Sheffield, UK, September, 2017. p. 244-249.

[8] Di Ludovico M, D'Ambra C, Prota A, Manfredi G. FRP confinement of tuff and clay brick columns: Experimental study and assessment of analytical models. J Compos Constr 2010; 14(5): 583-596.

[9] Minafò G, D'Anna J, Cucchiara C, Monaco A, La Mendola L. Analytical stress-strain law of FRP confined masonry in compression: Literature review and design provisions. Compos Part B-Eng. 2017; 115:160-9.

[10] Minafò G, Monaco A, D'Anna J, La Mendola L. Compressive behaviour of eccentrically loaded slender masonry columns confined by FRP. Eng Struct 2018; 172: 214-227.

[11] Aiello MA, Micelli F, Valente L. FRP confinement of square masonry columns. J Compos Constr 2009; 13(2): 148-158.

[12] Micelli F, Angiuli R, Corvaglia P, Aiello MA. Passive and SMA-activated confinement of circular masonry columns with basalt and glass fibres composites. Compos Part B-Eng 2014; 67: 348-362.

[13] Sandoli A, Ferracuti B, Calderoni B. (2019). FRP-CONFINED tuff masonry columns: Regular and irregural stone arrangement. Composites Part B: Engineering, 162, 621-630.

[14] Di Ludovico M, Fusco E, Prota A, Manfredi G. Experimental behaviour of masonry columns confined using advanced materials. In: The 14th world conference on earthquake engineering. October, 2008.

[15] Cascardi A, Micelli F, Aiello MA. FRCM-confined masonry columns: experimental investigation on the effect of the inorganic matrix properties. Constr Build Mater 2018; 186: 811-825.

[16] Minafò G, La Mendola L. Experimental investigation on the effect of mortar grade on the compressive behaviour of FRCM confined masonry columns. Compos Part B-Eng 2018; 146: 1-12.

[17] Carloni C, Mazzotti C, Savoia M, Subramaniam KV. Confinement of Masonry Columns with PBO FRCM Composites. In: Key Engineering Materials 2015. Vol. 624, p. 644-65. Trans Tech Publications Ltd.

[18] Murgo FS, Mazzotti C. Masonry columns strengthened with FRCM system: Numerical and experimental evaluation. Constr Build Mater 2019; 202: 208-222.

[19] Ombres L, Verre S. Masonry columns strengthened with Steel Fabric Reinforced Cementitious Matrix (S-FRCM) jackets: experimental and numerical analysis. Measurement 2018; 127: 238-245.

[20] Yilmaz I, Mezrea P, Ispir M, Binbir E, Bal I, Ilki A. External confinement of brick masonry columns with open-grid basalt reinforced mortar. In: Proceedings of the Fourth Asia-Pacific Conference on FRP in Structures (APFIS 2013). Melbourne, Australia, December, 2013. p. 11-13.

[21] Mezrea PE, Yilmaz IA, Ispir M, Binbir E, Bal IE, Ilki A. External jacketing of unreinforced historical masonry piers with open-grid basalt-reinforced mortar. J Compos Constr 2017; 21(3): 04016110.

[22] Fossetti M, Minafò G. Comparative experimental analysis on the compressive behaviour of masonry columns strengthened by FRP, BFRCM or steel wires. Compos Part B: Eng 2017; 112: 112-124.

[23] Santandrea M, Quartarone G, Carloni C, Gu XL. Confinement of masonry columns with steel and basalt FRCM composites. In: Key Engineering Materials 2017. Vol. 747, p. 342-349. Trans Tech Publications Ltd.

[24] Di Ludovico M, Cascardi A, Balsamo A, Aiello MA. Uniaxial experimental tests on full-scale limestone masonry columns confined with glass and basalt FRCM systems. J Compos Constr 2020; 24(5): 04020050.

[25] Ombres L, Verre S. Analysis of the Behavior of FRCM Confined Clay Brick Masonry Columns. Fibers 2020; 8(2): 11.

[26] Estevan L, Baeza FJ, Bru D, Ivorra S. Stone masonry confinement with FRP and FRCM composites. Constr Build Mater 2020; 237: 117612.

[27] Campione G, Miraglia N. Strength and strain capacities of concrete compression members reinforced with FRP. Cement Concrete Comp 2003; 25(1): 31-41.

[28] Krevaikas TD, Triantafillou TC. Masonry confinement with fiber-reinforced polymers. J Compos Constr 2005; 9(2): 128-135.

[29] Corradi M, Grazini A, Borri A. Confinement of brick masonry columns with CFRP materials. Compos Sci Technol 2007; 67(9): 1772-1783.

[30] Di Ludovico M, D'Ambra C, Prota A, Manfredi G. FRP confinement of tuff and clay brick columns: Experimental study and assessment of analytical models. J Compos Constr 2010; 14(5): 583-596.

[31] Italian Council of Research (CNR). CNR-DT 200 Guide for the design and construction of externally bonded FRP systems for strengthening existing structures. 2013.

[32] ACI (American Concrete Institute). 2013. Guide to design and construction of externally bonded fabric-reinforced cementitious matrix (FRCM) systems for repair and strengthening concrete and masonry structures, 1–69. ACI-549.4R-13. Farmington Hills, MI: ACI.

[33] Cascardi A, Longo F, Micelli F, Aiello MA. Compressive strength of confined column with Fibre Reinforced Mortar (FRM): New design-oriented-models. Constr Build Mater 2017a; 156: 387-401.

[34] Balsamo A, Cascardi A, Di Ludovico M, Aiello MA, Morandini G. Analytical study on the effectiveness of the FRCM-confinement of masonry columns. In: REHABEND 2018 Euro-American Congress on Construction Pathology, Rehabilitation Technology and Heritage Management, Cáceres, Spain, 2018. p. 1-9.

[35] Cascardi A, Aiello MA, Triantafillou T. (2017b). Analysis-oriented model for concrete and masonry confined with fibre reinforced mortar. Mater Struct 2017b; 50(4): 1-15.

[36] Micelli F, Maddaloni G, Longo F, Prota A. (2021). Axial stress–strain model for FRCM confinement of masonry columns. J Compos Constr 2021; 25(1): 04020078.

[37] D'Anna J. Experimental investigation on the effectiveness of basalt-fibre strengthening systems for confining masonry elements. (2019). PhD Thesis, XXXI Cycle, University of Palermo, Italy.

[38] D'Anna J, Amato G, Chen JF, La Mendola L, Minafò G. BFRP grid confined clay brick masonry cylinders under axial compression: experimental results. In: 9th International Conference on Fibre-Reinforced Polymer (FRP) Composites in Civil Engineering (CICE 2018). Paris, July, 2018. No. part 2, p. 123-129.

[39] D'Anna J, Amato G, Chen J.F, Minafò G, La Mendola L. Effectiveness of BFRP confinement on the compressive behaviour of clay brick masonry cylinders. Compos Struct 2020; 249: 112558.

[40] D'Anna J, Amato G, Chen J.F, Minafò G, La Mendola L. (2021). Performance assessment of basalt FRCM for the confinement of clay brick masonry cylinders. In: 12th International Conference on Structural Analysis of Historical Constructions (SAHC 2020). Barcelona, September 29-30, and October 1, 2021.

[41] EN 772-1. Method of test for masonry units – Part 1: Determination of compressive strength, 2011.

[42] EN 1015-11. Methods of test for mortar for masonry – Part 11: Determination of flexural and compressive strength of hardened mortar, 1999.

[43] ISO 13934-1. Textiles – Tensile properties of fabrics – Part 1: Determination of maximum force and elongation at maximum force using the strip method. CEN – European Committee for Standardization, April 2013.

[44] ICC. AC434. Proposed Acceptance Criteria for Masonry and Concrete Strengthening Using Fibre-reinforced Cementitious Matrix (FRCM) Composite Systems. Whittier, CA: ICC-Evaluation Service, 2013.

[45] GOM GmbH. GOM testing—technical documentation as of V8 SR1 digital image correlation and strain computation basics. 2016.

[46] Bisby LA, Chen JF, Li SQ, Stratford TJ, Cueva N, Crossling K. Strengthening fire-damaged concrete by confinement with fibre-reinforced polymer wraps. Eng Struct 2011; 33(12): 3381-3391.

[47] Balsamo A, Maddaloni G, Micelli F, Prota A, Melcangi G. (2018). Experimental behaviour of full scale masonry columns confined with FRP or FRCM systems. In: REHABEND 2018 Euro-American Congress on Construction Pathology. Rehabilitation Technology and Heritage Management, Cáceres, Spain, 2018.

[48] Incerti A, Vasiliu A, Ferracuti B, Mazzotti C. (2015, December). Uni-Axial compressive tests on masonry columns confined by FRP and FRCM. In: Proceedings of the 12th International Symposium on Fiber Reinforced Polymers for Reinforced Concrete Structures & The 5th Asia-Pacific Conference on Fiber Reinforced Polymers in Structures, Joint Conference.